

Medical needle steering for lung biopsy: experimental results in tissue phantoms using a robotic needle driver

Jienan Ding¹, Dan Stoianovici², Doru Petrisor², Pierre Mozer², Rick Avila³, Luis Ibanez³, Wes Turner³, David Yankelwitz⁴, Emmanuel Wilson¹, Filip Banovac¹, Kevin Cleary¹

¹Imaging Sciences and Information Systems (ISIS) Center, Department of Radiology, Georgetown University Medical Center, Washington, DC, USA {cleary@georgetown.edu}

²URobotics Laboratory, Department of Urology, John Hopkins Medicine, Baltimore, MD, USA

³Kitware Incorporated, Albany, NY, USA

⁴Weill-Cornell Medical Center, New York, NY, USA

Abstract - Needle steering is a commonly used technique in the medical field as it enables physicians to more precisely reach the target tissue. In this paper we describe our interest in needle steering for lung biopsy and the significance of this technique. There has been much interest in modeling needle steering in recent years and this paper builds upon that work. We describe our Matlab implementation and present simulation results. We also show our experimental results based on a robotic needle driver and X-Ray imaging in the interventional suite. The experimental results showed good agreement with the simulation results.

I. INTRODUCTION

Needle biopsy is an extremely common procedure in the medical field [1]. Many years of training and experience are typically required for physicians to master this skill. One technique often used by experienced physicians to guide the needle to the target is to steer the needle one way or the other. The needle deflection that can be achieved in soft tissue is affected by various factors such as needle stiffness, tip shape, and tissue properties.[2]. In particular, bevel tip needles are often used for needle steering.

The overall goal of this project is to develop a computer-aided system that can assist the radiologist in targeting small pulmonary nodules during CT-guided lung biopsy. The estimated 3D needle trajectory along with the range of potential needle trajectories given varying degrees of needle steering will be calculated and displayed to the radiologist Fig. 1. We believe that such an interactive guidance system can enhance the ability of the radiologist to successfully biopsy small nodules. Lung biopsy is an important clinical problem and the ability to successfully biopsy small nodules depends greatly on the skill of the physician. Small lung nodules are now being detected with increasing frequency and CT-guided transthoracic needle biopsy is the method of choice to obtain tissue for a pathologically confirmed diagnosis.

This is due primarily to increased indications to perform CT scanning, technologic advances in the scanner allowing for improved resolution, and increased availability of CT scanners. While there have also been improvements in the non-invasive diagnostic approach to evaluate these small CT

detected nodules, there continues to remain a subset where tissue is needed to achieve a pathologically confirmed diagnosis. With advances in molecular analysis it can also be anticipated that providing tissue specimens will become increasingly important as prognostic indicators. CT-guided transthoracic needle biopsy allows for this, and is minimally invasive compared to open surgery. However, the performance of this procedure is challenging for small nodules, and the ability to successfully perform the procedure decreases as the size of the nodules decreases. This is primarily due to the inability of the operator to guide the needle tip into the nodule. One of the main contributing factors to this is the difficulty the radiologist has in predicting the location of the needle tip prior to advancing it relative to the nodule. While this can be performed with relative ease for larger nodules when the needle and the nodule are both visualized in a single imaging plane, it is much more challenging for small nodules which may lie directly beneath a rib and thus require an angled approach such that the needle must cross through multiple scan planes. This project is intended to address this challenge by providing computer assistance in targeting these small pulmonary nodules.

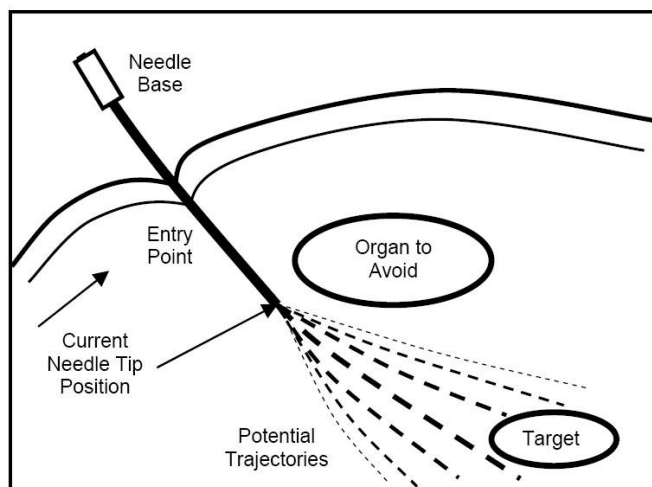


FIG. 1. PATH PLANNING FOR LUNG BIOPSY

In recent years, there has been much interest within the biomedical engineering community in modeling needle steering to improve biopsy accuracy. A nonholonomic kinematic model of needle steering was introduced by Webster et al. [3] and related papers have appeared from several other researchers. Dimaio developed a finite element model to simulate the needle and tissue properties [4]. Alterovtiz et al. introduced stochastic techniques to model the procedure [5]. Park et al. employed diffusion-based methods to the needle steering problem [6].

In this paper, we investigate the applicability of the nonholonomic model to robotically assisted needle placement based on a recently built robotic needle driver [7]. The needle steering component is part of a larger project on providing computer assistance for precision lung biopsy. Here we present a Matlab implementation of the nonholonomic model and our validation experiments using the robotic system.

The paper is organized as follows: Section II reviews the Matlab implementation and simulation results. Section III presents the experimental results using the robotic needle driver and x-ray fluoroscopy to visualize the needle path. Discussions and conclusions are given in Section IV.

II. SIMULATION RESULTS

A. Model and simulation platform

The nonholonomic model as presented by Webster et al [3] includes several parameters that must be experimentally determined, as described later in Section III.D of this paper. To implement this model, a Matlab program was developed with the GUI shown in Fig. 2. This GUI consists of the five component nonholonomic model fit, needle steering animation, potential field computation, monitor of needle status, and ability to save the needle status data.

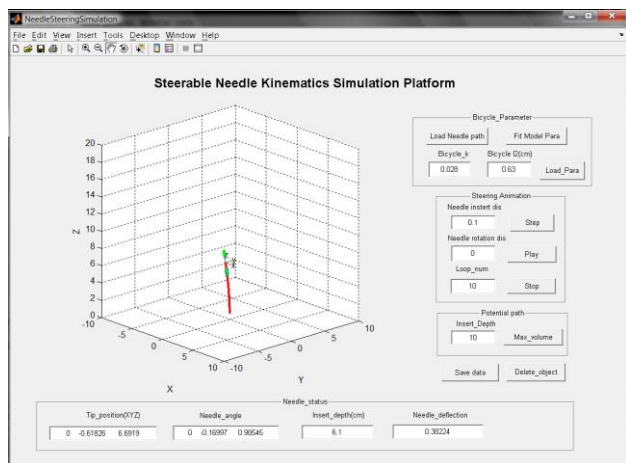


FIG. 2. SIMULATION PLATFORM GUI

B. Estimation curve

Fig. 3 shows three simulated needle trajectories generated by the nonholonomic model with parameters $k = 0.09$ and $l_2 = 2.7$ cm. These parameters were taken from the results shown in section III.D of this paper. In these curves, the dashed line

shows the needle insertion without any rotation, the dotted line shows the needle insertion with one 180° rotation, and the solid line shows the needle insertion with two 120° rotations. The needle was inserted to 10 cm depth in all cases. The results qualitatively agreed with previous simulations from the literature and therefore the next step was the phantom study described next.

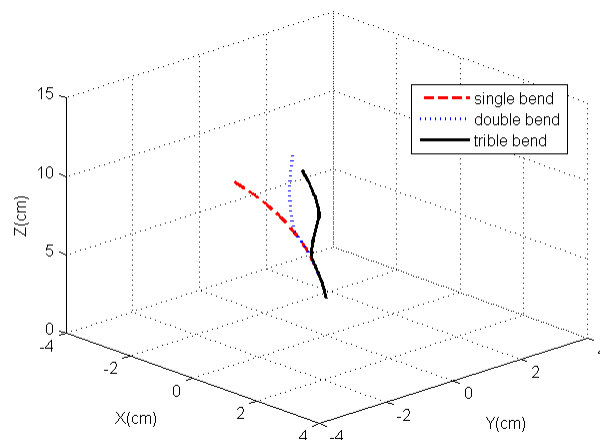


FIG. 3. NEEDLE SIMULATED TRAJECTORY

III. EXPERIMENTAL RESULTS

A. Materials

1) Phantom

Verification of the needle steering model was achieved through the use of a ballistic media phantom (SIM-TEST from Corbin Inc., White City, OR), shown in Fig. 4. The ballistic media was found to closely mimic muscular tissue properties. A standard biopsy needle (Westcott 22g x5 1/2 TW), 0.7 mm diameter and 45° bevel angle, was used for this experiment. A key assumption within the nonholonomic model is that the parameters defining the stiffness of the needle and tissue be close to each other. The stiffness of both the needle and phantom is approximately 4.9N/mm^2 .

Four spot fiducials were placed on the phantom surface for post CT image registration. Fig. 4 shows the phantom with fiducials and the biopsy needle.

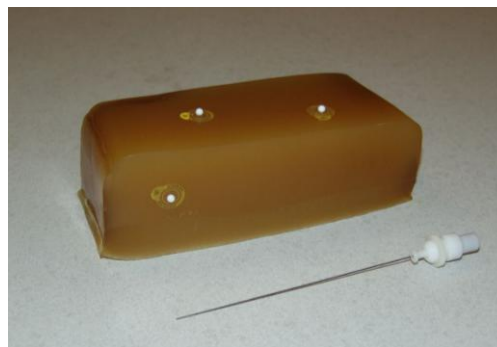


FIG. 4. PHANTOM, FIDUCIALS, AND BIOPSY NEEDLE

2) Acubot robot system

The robotic system used in these experiments is an updated version of the “AcuBot” system built by the Urology Robotics Laboratory at Johns Hopkins Medical Institutions [8]. The original AcuBot comprises the “PAKY” (Percutaneous Access of the KidneY) needle driver, the “RCM” (Remote Center of Motion) orientation module, and joystick control. A three degree of freedom Cartesian stage, passive position-S-arm, and “bridge frame” provide a compact and flexible design for interventions at multiple points along the body.

Prior experiences using the AcuBot system in clinical trials for spinal nerve blocks showed the need for some system enhancements [9]. The main focus of these enhancements was a complete redesign of the needle driver. Three new components were added to the needle driver: (1) a mechanism to spin the needle, (2) force sensors, and (3) a needle release mechanism. The updated system is referred to as the “AcuBot1 V2-RND” and shown in Fig. 5.

The compact RND holds the needle from two points for enhanced support and accurate insertions. This design prevents buckling of long thin needles. Moreover, it is capable of spinning the needle during insertion in either direction. Rotation of the needle may help to reduce the resistive forces by the “drilling effect.” Needle rotation may also be favorable by changing a higher static friction between tissue and needle to a lower kinetic friction thus reducing insertion forces. For these experiments, the rotational capability of the needle driver can be used to set the needle tip to any angle.

One unique feature of the needle driver is the built-in force sensing capability. A safety mechanism is also built into the needle driver to release the needle which can be triggered manually or upon a desired force level measured by the force sensors.

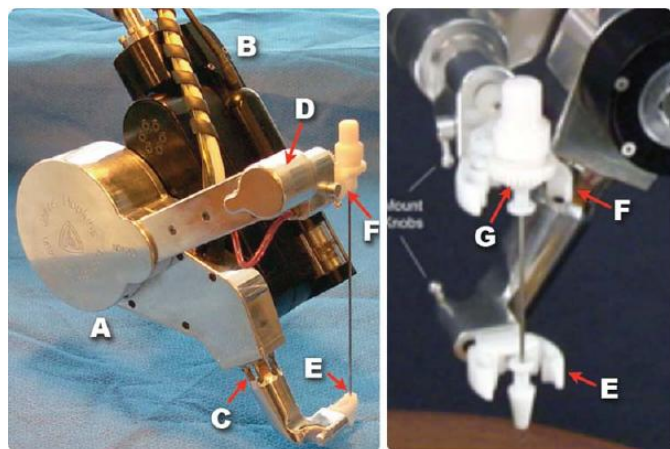


FIG. 5. ACUBOT ROBOT SYSTEM. (A) ROTATING NEEDLE DRIVER (RND), (B) REMOTE CENTER OF MOTION (RCM) ORIENTATION MODULE. (C)/(D) FORCE SENSOR, (E)/(F) HEAD AND BARREL GRIPPERS, (G) NEEDLE HUB

B. Method

The robot system was positioned in the Interventional Suite at Georgetown University Hospital as shown in Fig. 6. This suite includes the DynaCT Fluoroscopy System (Siemens

Medical Solutions) which provides a cone-beam CT capability to reconstruct tomographic images. The phantom was placed on the table and positioned within the imaging volume. The Acubot robot was placed beside the table and the needle was loaded into the rotating needle driver.



FIG. 6. ROBOT SETUP FOR EXPERIMENT

To verify the nonholonomic model, three sets of experiments were done. In case one, the rotation speed was set to zero, and the needle was inserted into the phantom to a depth of 100 mm with a translational speed of 5 mm/s. In case two, the needle was inserted 50 mm then stopped. The needle was then rotated 180 degrees and then inserted another 50 mm. In case 3, the needle was inserted 30 mm, followed by a 120 degree rotation, followed by another 30 mm insertion, followed by another 120 degree rotation, and then inserted 40 mm more. This third trial was intended to create an approximately 3D helical curve.

Each set of experiments was done four times for a total of 12 trials. After each trial, a DynaCT scan was done to provide a set of CT-like axial images from which the needle path could be reconstructed. The output images were saved in the DICOM medical image standard format.

C. Results

A fluoroscopic image of final needle placement for the second experiment is shown in Fig. 7. Since there was a great deal of artifact around the CT images, we were not able to segment the needle accurately using automatic techniques. Therefore, we used the public domain software ITK-Snap [10] to manually identify 25 points in each needle curve. We also manually identified the four registration fiducials.



FIG. 7. FLUOROSCOPY IMAGE OF FINAL NEEDLE POSITION WITHIN PHANTOM

Because we imaged the phantom after each needle placement, we had to move the DynaCT couch each time for this purpose. This also required moving the robot out of the way so that the C-arm could be rotated to acquire the cone beam CT images. In addition, the phantom was not rigidly fixed to the table and might have moved between each needle placement. For all of these reasons, we decided to register all 4 trials for each set of experiments into a common coordinate system so we could better compare the needle trajectory results. We used point based registration to minimize the linear least squares distance:

$$dis = \sum_{i=1}^N \left((x_i^s - x_i)^2 + (y_i^s - y_i)^2 + (z_i^s - z_i)^2 \right) \quad (1)$$

N is the points number in the needle, where (x_i^s, y_i^s, z_i^s) is the simulating curve and (x_i, y_i, z_i) is the needle curve from experiment.

D. Parameter kinematic Model

The nonholonomic model used here includes model parameters that must be experimentally determined. For this purpose, we used the Matlab function `nlinfit`. Here we used data from the four trajectories of experiment set one. The Matlab `nlinfit` function estimates the coefficients of a nonlinear regression function using a least squares methods.

Fig. 8. shows the results from the curve fitting. In this figure, the blue solid line is fit curve, dash redline marker by small spot is the mean values of four different needle trajectory. In addition, the confidence interval was drawn in this graph as a measure of the error.

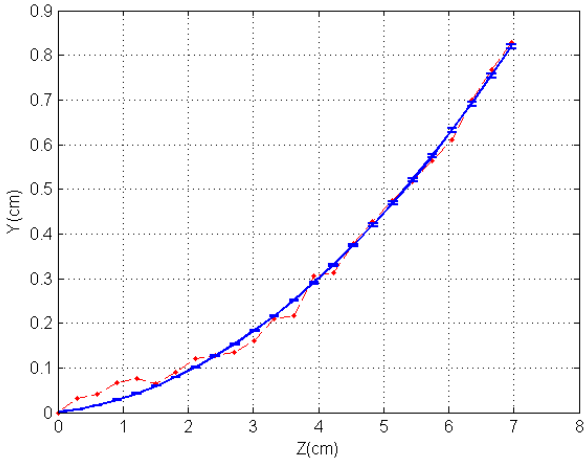


FIG. 8. CURVE FIT FOR EXPERIMENT SET ONE

E. Results

In the previous section, we computed the nonholonomic model parameters using the experimental trajectories for set one. This section quantifies the error between estimated and actual trajectories for sets two and three. Fig. 9. show the error for case two. The solid blue line is the estimated needle path, the dashed red line is the average position of four experimental needle placements. The error bar shows the

maximum and minimum needle trajectory. The overall results show relatively good agreement with the simulation.

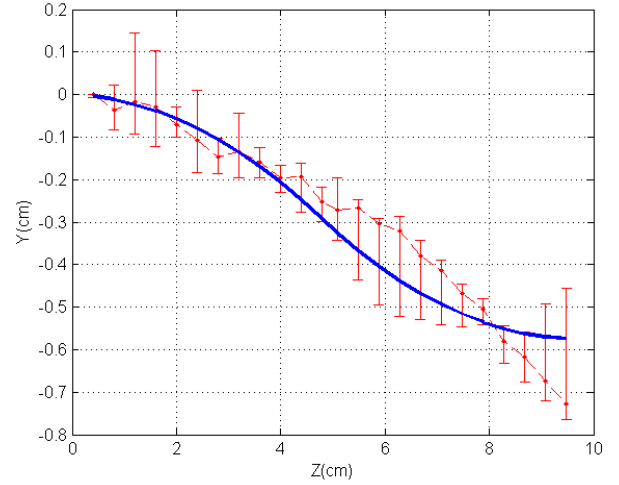


FIG. 9. ESTIMATED ERROR OF TWO BENDING CURVE

Fig. 9. shows the estimated error for experiment set three. The error values are indicated by the color of the triangle at each point. The estimated error close to the entry point was larger, because the entry point was different to identify in CT image. However, in general, the agreement with the simulation results was also considered good.

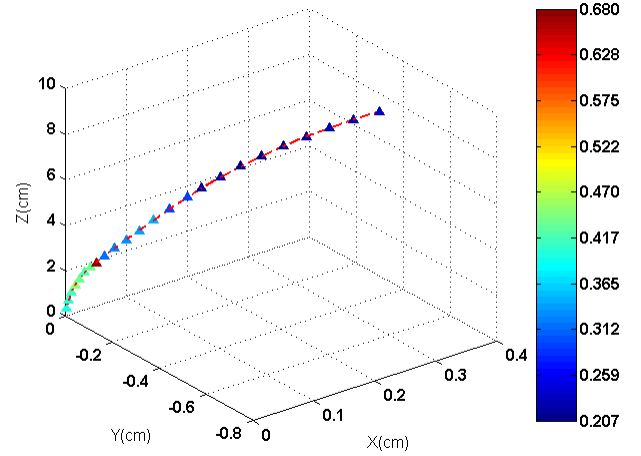


FIG. 10. ESTIMATED ERROR OF 3D NEEDLE CURVE

IV. CONCLUSION AND DISCUSSION

This paper first presented the nonholonomic model to estimate the trajectory of a steerable bevel-tip needle in soft tissue. Phantom results based on needle placement using a robotic needle driver were then show. The experimental results showed reasonable agreement with the simulation.

This is an initial study to investigate the applicability of needle steering toward lung biopsy of small pulmonary nodules. In future work, we hope to develop a computer aided system to assist the physician for more precise lung biopsies, including an estimation of possible needle deflection based on manipulating the biopsy needle.

V. ACKNOWLEDGMENT

This work was supported by a subcontract from Kitware Inc. as part of an NIH funded grant, R41 CA128214-01. The authors would like to thank Robert Webster of Vanderbilt University for his comments on a draft version of the manuscript.

reliability, *NeuroImage* Volume 31, Issue 3, , 1 July 2006, Pages 1116-1128.

VI. REFERENCE

- [1] Baumgarten, R. K, Importance of the needle bevel during spinal and epidural anesthesia, *Reg Anesth*, 1995,20(3),pp234-238
- [2] Sitzman, B. T. Uncles, D. R., The effects of needle type, gauge, and tip bend on spinal needle, *Anesth Analg*, 1996,82(2),pp 297-301
- [3] R. J. Webster III, J. S. Kim, N. J. Cowan, G. S. Chirikjian and A. M. Okamura, "Nonholonomic Modeling of Needle Steering," *International Journal of Robotics Research*, Vol. 25, No. 5-6, pp. 509-525, May-June 2006.
- [4] Simon P. Dimaio, *Needle Motion Simulation and Planning for Applications in Soft Tissues*, PhD dissertation, 2003, university of British Columbia
- [5] Ron Alterovitz, Michael Branicky, and Ken Goldberg, "Constant-Curvature Motion Planning Under Uncertainty with Applications in Image-Guided Medical Needle Steering," in *Proc. Workshop on the Algorithmic Foundations of Robotics*, Jul. 2006
- [6] Wooram Park; Jin Seob Kim; Yu Zhou; Cowan, N.J.; Okamura, A.M.; Chirikjian, G.S., "Diffusion-Based Motion Planning for a Nonholonomic Flexible Needle Model," *Robotics and Automation, 2005. ICRA 2005. Proceedings of the 2005 IEEE International Conference on* , vol., no., pp. 4600-4605, 18-22 April 2005
- [7] S. Shah, A. Kapoor, J. Ding, P. Guion, D. Petrisor, J. Karanian, W. F. Pritchard, D. Stoianovici, B. J. Wood, and K. Cleary, "Robotically assisted needle driver: evaluation of safety release, force profiles, and needle spin in a swine abdominal model," *International Journal of Computer Assisted Radiology and Surgery*, Volume 3, Numbers 1-2 / June, 2008, pp. 173-179.
- ¹ R. J. Webster III, J. S. Kim, N. J. Cowan, G. S. Chirikjian and A. M. Okamura, "Nonholonomic Modeling of Needle Steering," *International Journal of Robotics Research*, Vol. 25, No. 5-6, pp. 509-525, May-June 2006.[8]
- [8] Stoianovici D, Cleary K, Patriciu A, Mazilu D, Stanimir A, Craciunoiu N, Watson V, Kavoussi L (2003) Acubot: a robot for radiological interventions. *IEEE Trans Robot Autom* 19(5):927-930
- [9] Cleary K, Watson V, Lindisch D, Taylor RH, Fichtinger G, Xu S, WC S, Donlon J, Taylor M, Patriciu A, Mazilu D, Stoianovici D (2005) Precision placement of instruments for minimally invasive procedures using a "Needle Driver" robot". *Int J Med Robot* 1(2):40-47
- [10] Paul A. Yushkevich, Joseph Piven, Heather Cody Hazlett, etc, User-guided 3D active contour segmentation of anatomical structures: Significantly improved efficiency and